DV-80-9 No. 3

INFILTRATION-PRESSURIZATION CORRELATION: SIMPLIFIED PHYSICAL MODELING

DR. MAX H. SHERMAN
Student Member ASHRAE

DR. DAVID T. GRIMSRUD
Member ASHRAE

ABSTRACT

In this paper we present a model for predicting air infiltration that eliminates many site-specific parameters normally required. The only information necessary is the geometry and leakage of the structure. The leakage quantities, expressed in terms of effective areas, are total leakage area and the leakage areas of the floor and ceiling. Weather parameters are mean wind speed, terrain class, and average temperature difference. The model separates the infiltration problem into two distinct parts: stack and wind-regimes. Each regime is treated independently; the transition between them is sharp. The model has been tested with data from several sites, differing in climate and construction methods.

INTRODUCTION

Understanding the infiltration process is critical to any residential conservation program in as much as infiltration is a primary source of energy loss in residences. Yet we are far more capable of calculating conduction losses than losses due to infiltration. Several explanations for this disparity can be cited. First, conduction losses are more easily calculated because the heat transfer is proportional to the temperature difference and does not depend strongly on any other driving force. Infiltration, on the other hand, depends on the interior-exterior pressure difference but is not simply proportional to it. Furthermore, the driving pressure is caused by uncorrelated physical effects (wind speed and temperature difference). Second, conduction losses can be characterized by means of one parameter, the thermal resistance; infiltration, until now, has had no equivalent quantity. We propose in this paper that an appropriate parameter for characterizing the infiltration loss is the effective leakage area.

M.H. Sherman, D.T. Grimsrud

Energy and Environment Division, Lawrence Berkeley Laboratory, University of California, Berkeley, Ca. 94720

The work described in this report was funded by the Office of Buildings and Community Systems, Assistant Secretary for Conservation and Solar Applications of the U.S. Department of Energy under contract No. W-7405-Eng-48.

It is because of these problems that infiltration has been a difficult quantity to model. Previous attempts at modeling infiltration have used statistical fitting [1-3] or have involved measurements or calculations that are too difficult to make on a large scale.[4] This paper introduces a model that sacrifices accuracy for versatility and simplicity. Rather than predicting accurately the weather induced infiltration of a particular structure, the model is designed to calculate the infiltration of a general structure. Furthermore, the model predicts the impact of retrofits or other changes in the building envelope on the basis of performance changes effected in a few measurable parameters.

The parameters used in the model are:

1) The leakage area(s) of the structure.
   The leakage area is the parameter that describes the tightness of the structure (obtained by pressurization). Most retrofits will affect the leakage area or the leakage distribution.

2) The height of the structure.
   The height and other geometric quantities are usually known or can be directly measured.

3) The inside-outside temperature difference.
   The temperature difference gives the magnitude of the stack effect. It is also necessary for the calculation of the energy load due to infiltration.

4) The terrain class of the structure.
   The terrain class of the structure is a description of the density of other buildings and obstructions which influence the dependence of wind speed on height near the structure. Knowing the terrain class of the structure allows the use of off-site weather data for the calculation of wind-induced pressures.

5) The wind speed.
   The wind speed is required to calculate the wind-induced infiltration for comparison with the stack effect.

The wind speed used by the model can be calculated from a wind speed measured on any weather tower in the area. Using standard wind formulas (cf. Table A1) the wind speed in any terrain class and at any height can be converted to the wind speed at the site. Thus, on-site weather collection is not necessary in our model. We must emphasize, however, that the measured wind data must be for the "same wind", i.e. there can be no mountain ranges or other major terrain disturbances between the site and the wind tower.

AIR LEAKAGE

Air leakage is the simple process of air passing through normal openings or cracks in the structure. These openings range in size from those of undampered vents (about 0.2m) to tiny cracks around windows (about 0.2mm).

As we know from hydrodynamics, the character of the air flow through a leakage opening changes as the pressure across the opening changes. At very low pressures, the flow is dominated by viscous forces; at high pressures, by inertial forces. Therefore, at low pressures we expect the flow to be proportional to the applied pressure and at high pressures we expect the flow to be proportional to the square-root of the applied pressure. At intermediate pressures the behavior will be a mixture of these effects.

The pressure range in which the flow behavior changes depends on the geometry of the individual crack. While good data[5] exist describing the functional form for an individual crack, the leakage characteristic of the entire structure is much harder to model. The flow vs pressure curve of the structure will be the summation of all of the individual crack curves. Since it is impossible to know the geometry of each crack, calculating the flow vs pressure curve of a real structure cannot be done from first principles.

Field measurements[6-9] have shown that the behavior of the actual leakage curve more closely resembles that expected for turbulent flow than for viscous flow in the pressure region typical of the pressures which drive infiltration. These findings indicate that the transition pressure (where the flow changes from viscous to turbulent) is below the experimental range. Therefore, in our model, we assume flow to be proportional to the square-root of the applied pressure.

$$Q = A \sqrt{\frac{2}{\rho} \Delta P} \tag{1}$$

where

Q is air flow (m^3/sec),

A is the effective leakage area (m^2),

ρ is the density of air (1.2 kg/m^3) and

ΔP is the applied pressure (Pa).

It is the effective leakage area that characterizes the air leakage. In subsequent discussion we refer to this simply as the leakage area.

In an actual structure there are many leakage sites, each having a leakage area. In this model we combine the leakage sites into three areas: A_o is the total leakage area of the structure (the sum of the leakage areas of the floor, walls and ceiling), A_f is the leakage area of the floor, and A_c is the leakage area of the ceiling.

As will be shown in the Appendices, it is necessary to differentiate the floor and ceiling leakages from the total leakage area because the stack and wind pressures influence these locations differently.

Leakage Measurement

Air leakage is usually measured by fan pressurization.[4] This technique uses a large-capacity fan to push air either into or out of the structure. Flow continuity requires that all the air that flows through the fan must flow out through the building shell. The flow, measured as a function of the pressure drop across the envelope, is called the leakage curve of the building.

In general, leakage curves obtained by this method will not be proportional to the square-root of the pressure drop across the envelope. Our model assumes that it is, however, and so we extrapolate the leakage curve (if necessary) down into the pressure range of natural weather effects (0-10 Pa). We then fit the leakage curve to a square-root in that region. The fitting procedure gives us the total leakage area of the structure.

Example: Assume that through fan pressurization tests the following flow vs pressure data have been measured:

ΔP (Pa)	10	20	30	40	50
Q (m^3/hr)	800	1220	1560	1850	2110

Unlike walls, floor and ceiling surfaces have few penetrations. Once they are located a their physical dimensions measured, the leakage area (usually smaller than the physical area the opening) can easily be calculated by estimating the discharge coefficient from the dime sions of the leak. Various references including the ASHRAE Handbook of Fundamentals conta tables or formulas for discharge coefficients. In cases where a floor or ceiling is made materials that cannot leak (e.g., a slab floor), its leakage area may be assumed to be zero.

Finally, it is possible to assume a value for leakage not accounted for by measurement calculation. For example, this can be done by assuming that the amount of leakage per un shell area is the same for all surfaces.

INFILTRATION MODEL

In Appendix A we derive a general theory of infiltration. This derivation includes numero physical parameters and is useful mainly for large computer programs (e.g., DOE-2). We ha reduced the complexity of the model and the number of on-site measurements by introducing a s of simplifying assumptions, which are described in Appendix B.

In this model, we assume that the structure is a single well-mixed zone; we use typic shielding values for a simple rectangular structure; we neglect terms that depend on the si of the temperature difference. Most importantly, we split the problem into two distinct part the wind-regime, where the dynamic wind pressure dominates the infiltration; and the sta regime, where the temperature difference dominates the infiltration. Infiltration in the t regimes is expressed as follows:

$$Q_{wind} = f_w A_o v \qquad (2.1$$

$$Q_{stack} = f_s A_o \sqrt{2gH \frac{\Delta T}{T}} \qquad (2.$$

where

Q_{wind} is the infiltration in the wind-regime (m^3/sec),
Q_{stack} is the infiltration in the stack regime (m^3/sec),
v is the wind speed at ceiling height (m/sec),
ΔT is the inside-outside temperature difference (^oK),
g is the acceleration of gravity (9.8 m/sec^2),
H is the height of the ceiling above grade (m) and
T is the inside temperature (^oK).

Definitions for f_w and f_s are presented in Appendix B.

$$f_w = \frac{3 - R}{9} \qquad (3.$$

$$f_s = \frac{2 + R}{9} \qquad (3.$$

R is the fraction of the effective leakage that is horizontal (i.e. the sum of the floor a ceiling leakage divided by the total leakage).

$$R = \frac{A_c + A_f}{A_o} \qquad (4$$

The wind speed used in the equations above is the effective wind speed at ceiling height -- that is, the wind speed that would exist at the height of the ceiling if the building and its immediate surroundings were not there. The ceiling height is defined as the height (above grade) of the attic floor. In the case of raised foundations the total height of the living space may be different from the height of the attic floor above grade; however, we ignore this difference in our derivation. This wind speed can be calculated from any measurement of the same wind using the following formula,

$$v = v' \left[\frac{\alpha \left(\frac{H}{10} \right)^{\gamma}}{\alpha' \left(\frac{H'}{10} \right)^{\gamma'}} \right] \tag{5}$$

<u>where</u>

v' is the measured wind speed (from a weather tower)

H is the height of the ceiling,

H' is the height of the wind measurement,

α, γ are empirical constants given in Table A1.

The unprimed quantities refer to the structure site and the primed quantities refer to the wind-measurement site.

We have treated the intermediate regime (between stack and wind) by extrapolating the stack- and wind-regime formulae until they cross; thus, the predicted infiltration will be the larger of the two.

$$Q(\Delta T, v) = \text{MAX}(Q_{wind}, Q_{stack}) \tag{6.1}$$

$$= A_o \, \text{MAX}(v^*, v_s^*) \tag{6.2}$$

Where the starred (reduced) quantities are defined as,

$$v^* = f_w v = v' f_w^* \tag{7.1}$$

$$f_w^* = \frac{3 - R}{9} \left[\frac{\alpha \left(\frac{H}{10} \right)^{\gamma}}{\alpha' \left(\frac{H'}{10} \right)^{\gamma'}} \right] \tag{7.2}$$

$$v_s^* = f_s v_s = \sqrt{\Delta T} \, f_s^* \tag{8.1}$$

$$f_s^* = \frac{2 + R}{9} \sqrt{\frac{2gH}{T}} \tag{8.2}$$

Because the reduced stack and wind parameters (starred f's) in the above equations are weather-independent, they need be calculated only once for a given structure. We have calculated the reduced parameters for a special case -- <u>i.e.</u>, when the terrain class of the structure is the same as that for the wind measurement, and when the height of the wind measurement is 10 meters. This is the most common case, principally because most wind measurements are made with a 10-m weather station on-site. Table 1 contains values of the reduced stack parameter as a function of the height of the structure and the fraction of leakage in the floor and ceiling. Tables 2.1 to 2.5 contain the values of the reduced wind parameter as a function of the height of the structure and the fraction of the leakage in the floor and ceiling for the five terrain classes.

Having completely separated the weather-dependent parts from the weather-independent parts, we were able to devise a single graph that allows the infiltration of any structure to be calculated in any weather condition (see Figures 1 and 2).

Description of Figures 1 and 2.

Either Fig. 1 or Fig. 2 can be used to predict the infiltration of a particular site under any given weather condition using a few simple steps. Refer to the symbol table and list of defining relations that precede the figures for the terms used below.

1) From leakage measurements, determine A_o, A_c, and A_f. These, in turn, determine the fraction of leakage in the floor and ceiling, R. R is then used to calculate f_w and f_s.

2) The height of the structure, H, and the internal temperature, T, are combined with the stack parameter, f_s, to give the reduced stack parameter, f_s^*. Table 1 can be used to give the reduced stack parameter for the special case of on-site weather collection at 10 m.

3) The ceiling height of the structure and the height of the weather tower are combined with the terrain classes of the two sites and the wind parameter, f_w, to give the reduced wind parameter, f_w^*. For the special case of on-site weather collection at 10 m, Table 2 can be used to give the reduced wind parameter.

4) The wind speed, v', can be combined with f_w^* to give v^* and the inside-outside temperature difference, ΔT, can be combined with f_s^* to give v_s^*.

The combination of v^* and v_s^* define a point on the graph. That point falls on one of the constant infiltration lines. The axes of the graphs are in metric units; the number read from the constant infiltration lines has units of $m^3/hr/cm^2$. To find the actual infiltration in cubic meters per hour, that number should be multiplied by the total leakage area in centimeters squared (cm^2).

Steps 1-3 need be done only once per structure unless the leakage area of the structure is changed. Step 4 is necessary only if Fig. 2 is used, because Fig. 1 uses the reduced and weather parameters directly.

RESULTS

Fifteen different sites were extracted from the literature to represent a large spread in climate type, house construction type and measured infiltration rates.[10-12] In all cases, leakage data obtained by fan pressurization were available, permitting us to calculate the effective leakage area. (Note that the effective leakage area varies over a factor of 16 from tightest to loosest.) The fraction of leakage in the floor and ceiling and the terrain parameters were estimated from the qualitative description of each site. In Table 3, the effective leakage area, the reduced parameters, and the house volumes are presented for each site.

For most of the sites, the data consist of several short-term infiltration measurements made on a single day. Most infiltration measurements were made by using a tracer decay technique[4] which finds the average infiltration over a period of about an hour with a 5%-10% accuracy. For each measured infiltration point, a predicted infiltration was calculated from the weather variables and house parameters. Figs. 3 and 4 contain the plots of predicted vs measured infiltration.

Since the set of data for each site was taken on the same day, we have combined the sets to find an average measured infiltration and an average predicted infiltration for each site. Table 2 contains these average infiltrations as well as the average weather variables from which the predicted infiltration was calculated, together with their associated standard errors.

DISCUSSION

Considering the simplicity of the model and the fact that there are no adjustable parameters, the agreement is good. However, there are a few sites that do not have particularly good agreement; some over-predict and some under-predict. In order to explain some of these discrepancies, we examined other factors that may affect the infiltration.

Site 15 (Southampton) was the leakiest of all the sites and proved to be an under-predictor. At the time we were measuring infiltration in this house, the furnace fan was on. Because the ducts run through unconditioned spaces, any leakage in the ducts means that part of the air circulated by the furnace fan will exfiltrate causing an increase in infiltration. This increase is not accounted for by our model.

Site 10 (Neilson), also one of the leakiest houses measured, showed significant under-prediction as well. Because this house had no chimney damper, the wind blowing over the chimney caused a net suction on the house. If there were a damper or glass doors on the fireplace, the effect of this suction would have been minimal; with no obstruction to the flow, however, exfiltration increased and could not be accounted for by our model.

One of the crudest assumptions we have made is that the shielding coefficients can be assumed to be those of an exposed rectangular structure. For structures that have significant local shielding, we might expect the measured infiltration to be lower than the predicted infiltration. Without precisely quantifying the degree of shielding at each site, we examined the description of all the structures and found three sites (9, 13 and 14) that were heavily shielded and two sites (2 and 8) that were very heavily shielded.

For the very heavily shielded sites the data clearly show that the model over-predicts the infiltration by a factor that approaches two. Of the heavily shielded sites, Site 13 (Fels) over-predicts by an average of 50%, Site 9 (Purdue) over-predicts by an average of 25%, and Site 14 (San Carlos) under-predicts by an average of 15%.

The case of site 14 is unique in that it was the only site to be heavily shielded and also have an undampered chimney. These two effects tend to counterbalance each other; however, in any given situation (depending on wind speed and direction) one could easily outweigh the other. The data from this site reflect this variability. In one case, the predicted infiltration is well below the measured infiltration, suggesting that the chimney has a substantial effect. In the other three cases, the predicted infiltration is slightly above the measured infiltration, suggesting that the excess shielding is playing an important role.

While the accuracy of the model is sufficient for a wide variety of applications, the shortcomings described above suggest ways in which accuracy can be improved. Not only can we include new parameters to account for local shielding, but we can extend the model to account for stack flows through vents and flues and for active systems (furnace fans) all of which may interact with natural ventilation.

Retrofit Evaluation

Infiltration depends on the leakage area in two different ways: (1) it scales linearly with the total leakage area and (2) the f's depend weakly on the fraction of the leakage in the floor and ceiling. In general a single retrofit will make only a small change in the leakage area of the structure; hence, we can ignore the effect that a particular retrofit will have on the f's. The impact of a retrofit in changing infiltration is proportional to the change it effects in the total leakage area. (It should be noted that the model is more accurate in predicting changes in infiltration due to changes in the leakage area than in predicting absolute infiltration. Accordingly, to evaluate the effect of a retrofit on infiltration requires simply an evaluation of its effect on the leakage area. We suggest that a list of leakage areas be compiled for various architectural components to aid in predicting infiltration savings. The effective leakage area of each component becomes a powerful tool for predicting energy losses due to infiltration.

CONCLUSION

We have introduced the concept of leakage area as the characteristic quantity associated with infiltration, just as conductivity is the characteristic quantity associated with conduction. Using this concept, we have devised a model for predicting the infiltration based on a few easily determined physical parameters. Houses of widely different construction types and located in varying climatic conditions can be measured and compared by means of this model, in as much as all of the parameters used (i.e. leakage areas, terrain classes etc.) have physical reality outside of our model and, therefore, are independently measurable.

In future studies, we will explore long-term average infiltration data from a number of dissimilar sites to test the overall scale of the model. In addition, we will measure infiltration before and after retrofit, comparing the predicted infiltration reduction based on our model with the actual infiltration reduction measured based on tracer gas measurements.

APPENDIX A: Derivation of basic model

In this appendix the basic physical model of infiltration will be derived. This model is similar to a previously presented model[13] with one exception: in the prior model we assumed linear (viscous) flow through cracks as the dominant leakage mechanism, while in this work we generalize the concept to allow the flow through a crack to be proportional to the applied pressure raised to an arbitrary power.

First, we separate out the effects of the driving force of the structure (air leakage) by using the intermediary of surface pressures; knowledge of the terrain and weather allows surface pressures to be calculated. Second, we combine the surface pressures with the leakage function (and geometry) to calculate infiltration. In the following sections, we will combine these two operations into a complete description of weather-driven infiltration.

General Leakage Model

Air leakage is the natural flow of air through cracks, holes, etc. across the building envelope. There are two physically well-defined types of air flow: viscous and turbulent. In the viscous regime, the flow is proportional to the applied pressure; in turbulent flow, the flow is proportional to the square-root of the applied pressure. The type of flow is determined by the applied pressure and the crack geometry. In most houses there will be air flows in both regimes as well as in transition between regimes. A popular way of expressing this fact is to assume that the air flow is proportional to the applied pressure raised to some power between 1/2 and 1, and then to find the parameters experimentally.

$$Q(\Delta P) = L\,\Delta P^{n} \tag{A1}$$

where

Q is the air flow due to an applied pressure, (m^3/sec)

ΔP is the applied pressure, (Pa)

L, n are semi-empirical constants.

In an actual structure, the leakage may depend on the sign of the applied pressure and will also be different on different faces of the structure. To account for these possibilities, we further generalize the above expression to

$$Q_j^+ = L_j^+\,(\Delta P_j^+)^{n_j^+} \tag{A2.1}$$

$$Q_j^- = L_j^-\,(\Delta P_j^-)^{n_j^-} \tag{A2.2}$$

where

- j is the index to denote each face of the structure,
- $+$ indicates depressurization
- $-$ indicates pressurization.

Surface Pressures

Differential pressures on a structure are caused by the stack effect and the wind effect. The stack effect is the change in pressure due to a change in the density of two bodies of air which, in turn, is caused by a temperature difference between the two air masses. The size of this effect is given by the stack pressure,

$$P_s = \rho\, g\, H \frac{\Delta T}{T} \tag{A3}$$

where

- P_s is the stack pressure,
- ρ is the density of air, (1.2 kg/m^3)
- g is the acceleration of gravity (9.8 m/sec^2)
- H is the height of the structure (m)
- ΔT is the inside-outside temperature difference (^{o}K) and
- T is the inside temperature ($\simeq$295 ^{o}K).

The change in pressure with respect to height can be calculated by the following equation

$$\frac{d\Delta P}{dh} = -\frac{P_s}{H} \tag{A4}$$

where

- ΔP is the outside-inside pressure drop and
- h is the height from floor level

The minus sign comes from our definition of the relative signs of ΔT and ΔP.

The wind effect is an exterior pressure caused by a stream of air impinging upon a stationary object. The dynamic pressure caused by a wind striking a fixed object is called the stagnation pressure.

$$P_{st} = \tfrac{1}{2}\, \rho\, v^2 \tag{A5}$$

where

- P_{st} is the stagnation pressure and
- v is the wind speed.

We can define a dimensionless measure of the wind strength relative to the stack pressure.

$$\sigma = \frac{P_{st}}{P_s} = \frac{v^2}{2gH} \frac{T}{\Delta T} \tag{A6}$$

where

σ is the wind strength*

Wind Speed

The definition of wind speed is important in determining infiltration. We define the wind speed, v, to be the wind speed at the height of the ceiling of the structure if the structure and immediate surroundings were not there. Thus, in our definition of wind speed, we are excluding any effects of the local environment. However, because of the nature of wind dynamics, the wind speed measured at one height in one type of terrain will not be the same as the wind speed measured at another height or in another type of terrain.

To account for this variability, we use a standard formula[14] to calculate the wind speed at any height and terrain class from the wind speed at any other height and terrain class.

$$v = v_o \, \alpha \left(\frac{H}{10} \right)^{\gamma} \tag{A7}$$

where

- v is the actual wind speed
- v_o is the wind speed at standard conditions
- α, γ are constants that depend on terrain class

To calculate the wind speed at one site from measured data at another site, we first use the above formula to calculate the standard wind speed for the measurement site; then the standard wind speed is used to calculate the wind speed at the desired site. Values for the two terrain class-dependent parameters are shown in Table A1.

We must take into account the effect of the local terrain on the wind pressures felt by the structure. We do this by introducing shielding coefficients* that convert the stagnation pressure into the actual pressure felt by the exterior of the structure. Full-scale studies[15] have shown that the pressure distribution on flat faces can be adequately described by using the average pressure on the face. Accordingly, there is one shielding coefficient for every face of the structure.

$$\Delta P_j^w = C_j \, \tfrac{1}{2} \rho v^2 = C_j \, \sigma \, P_s \tag{A8}$$

where

- ΔP_j^w is the exterior pressure rise due to the wind and
- C_j is the shielding coefficient for the jth face.

The shielding coefficients must be functions of the angle between the incident wind and the orientation of the structure. Since we will eventually average the shielding coefficients over angle, we have suppressed their explicit dependence of them on angle.

---

*Our wind strength parameter is similar to other dimensionless quantities such as the Archimedes number. Specifically, the wind strength, σ, is equal to the reciprocal of twice the square of the Archimedes number.

* The term shielding coefficient is equivalent to the more standard term of exterior pressure coefficient; the only difference lies in the interpretation. We use the term shielding coefficient to mean the ratio of the average exterior wind pressure to the stagnation pressure at the ceiling height.

Combining Stack and Wind Effects

Now that we have expressions for both the stack and wind effects, we can combine them to find the total pressure drop across each face of the structure.

$$\Delta P_j = \Delta P_o - P_s \frac{h}{H} + C_j \; \tfrac{1}{2} \rho v^2 \tag{A9}$$

where

ΔP_j is the pressure drop across the jth face and

ΔP_o is the internal pressure change

The internal pressure change is the shift in internal pressure due to weather. It is determined by the condition that the air flow into the structure must balance the air flow out of the structure. To simplify this expression we make the following definitions:

$$\beta = \frac{h}{H} \tag{A10.1}$$

$$\Delta P_\sigma = P_s \beta^o - C^o \; \tfrac{1}{2}\rho v^2 \tag{A10.2}$$

$$\beta_j = \beta^o + \sigma (C_j - C^o) \tag{A10.3}$$

where

β is a dimensionless height,

β^o is called the neutral level,

β_j is called the effective neutral level of the jth face and

C^o is called the internal pressure coefficient

At this point the neutral level and internal pressure coefficients must be regarded as arbitrary functions of weather but, as will be demonstrated in Appendix B, for most purposes they may be treated as constants. Note also that when there is no wind ($\sigma = 0$) the effective neutral levels are equal to the neutral level.

Combining all this together, we get a deceptively simple expression for the pressure drop across the envelope:

$$\Delta P_j = P_s (\beta_j - \beta) \tag{A11}$$

COMBINING SURFACE PRESSURES AND AIR LEAKAGE

Now that we have expressions both for the surface pressures acting on the structure and the response of the structure to these pressures, we can derive an expression for the infiltration. We must be careful, however, to separate exfiltration (which is driven by negative differential surface pressures) and infiltration (which is driven by positive differential surface pressures). We must integrate the leakage expression over the entire surface and sum the infiltration and exfiltration separately. The results of these calculations are presented in Table A2, below.

There are three different types of structure faces to be considered: floor, walls and ceiling. Because the floor and ceiling are both at a constant height, the integration over height is trivial; there can be infiltration or exfiltration through one of them but not both. The walls, being vertical, may have both infiltration and exfiltration if the effective neutral level is between the floor and the ceiling. We split the problem up into three cases, depending on the value of the effective neutral level:

1) The effective neutral level is above the ceiling.
   $(1 < \beta_j)$

2) The effective neutral level is between the floor and the ceiling.
   $(0 < \beta_j < 1)$

3) The effective neutral level is below the floor.
   $(\beta_j < 0)$

The combination of three faces, three neutral level positions and two air flow directions yields 18 entries for Table A2.

This analysis assumes knowing a host of structural site-specific parameters (L's, n's, C's). Additionally, the calculation of infiltration changes form depending on the value of the effective neutral level. These factors would make the calculation of infiltration very tedious and hence impractical for a large number of sites. In Appendix B, we show how the model can be simplified by making certain reasonable physical assumptions.

APPENDIX B: Simplified analysis

The purpose of this section is to present a simplified expression for the infiltration rate of a structure. We will make reference to the general theory of air infiltration, and apply many approximations. Along the way, the approximations will be explicitly stated as they are made.

APPROXIMATION 1: The flow is dominated by simple orifice flow

Recent evidence[7] indicates that even at low pressures the flow through a structure is dominated by turbulent flow. That is, viscous forces do not appear to dominate the air leakage at typical weather-induced pressures. The turbulent case is equivalent to restricting the values of the L's and n's used in the general model.

$$L_j^+ = L_j^- = A_j \sqrt{\frac{2}{\rho}} \tag{B1.1}$$

$$n_j^+ = n_j^- = 1/2 \tag{B1.2}$$

where

A_j is called the effective leakage area of the jth face (m^2).

In terms of the air flow through a structure face,

$$Q_j = A_j \sqrt{\frac{2}{\rho} \Delta P_j} \tag{B2}$$

where

Q_j is the flow through the jth leakage site,
ΔP_j is the pressure drop across the jth site.

APPROXIMATION 2: The floor and ceiling are well shielded

In most circumstances the wind pressure felt by the floor and ceiling is much smaller than that felt by the walls; therefore, we will set the shielding coefficients of the floor and ceiling arbitrarily to zero.

We are now in a position to rewrite Table A2 using our approximations. Before doing so, we will change nomenclature slightly. The subscript j refers to any of the structural faces; we introduce the subscript w which is restricted to the walls of the structure only. We also define the critical velocity, v_s, to be the velocity of the wind when the stack pressure equals the stagnation pressure.

$$v_s = \sqrt{2gH\frac{\Delta T}{T}} = \frac{v}{\sqrt{\sigma}} \tag{B3}$$

where

v_s is the critical velocity.

Table B1 presents the expressions relating the infiltration to the weather parameters under these assumptions.

APPROXIMATION 3: The infiltration can be split into two regimes.

Even though we have simplified the problem, we cannot yet calculate infiltration directly. To calculate the infiltration we split the problem into two halves: wind-dominated and stack-dominated regimes. We assume that either all of the effective neutral levels are between the floor and the ceiling or none of them are. If all of the effective neutral levels are between the floor and the ceiling ($0<\beta_j<1$) then infiltration is stack-dominated; if all of them are above the ceiling ($1<\beta_j$) or below the floor ($\beta_j<0$) then it is wind-dominated. The derivation for both cases is shown below.

Stack Regime

In the stack regime we require the effective neutral level to be between the floor and the ceiling ($0<\beta_j<1$). Extracting these lines from Table B1 and summing the infiltration and exfiltration, we have:

$$Q^{+} = v_s\left[A_f\sqrt{\beta^o - \sigma C^o} + \frac{2}{3}\sum_w A_w(\beta^o + \sigma(C_w - C^o))^{3/2}\right] \tag{B4.1}$$

$$Q^{-} = v_s\left[A_c\sqrt{1 - \beta^o + \sigma C^o} + \frac{2}{3}\sum_w A_w\left(-\beta^o - \sigma(C_w - C^o)\right)^{3/2}\right] \tag{B4.2}$$

where

Q^{+} is the infiltration and

Q^{-} is the exfiltration.

APPROXIMATION 4: The neutral level is about half way up the structure.

The neutral level, β^o, represents the level at which the indoor-outdoor pressure difference is zero when there is no wind. Above the neutral (pressure) level, the indoor pressure is larger, causing exfiltration; below, the indoor is smaller than the outdoor pressure and infiltration occurs. The height of the neutral level in a structure will be about half the height of the structure. To examine the dependence of the infiltration on position of the neutral level, we expand expressions which contain the height of the neutral level about the point $1/2$ (times the structure height). We define a quantity, μ, to be the deviation from that point ($\beta^o = 1/2$).

$$\mu = \beta^o - 1/2 \tag{B5}$$

We then rewrite the equations for the infiltration and exfiltration sums as:

$$Q^+ = v_s\left[A_f(1/2 + \mu - \sigma C^o)^{1/2} + \frac{2}{3}\sum_w A_w(1/2 + \mu + \sigma(C_w - C^o))^{3/2}\right] \tag{B6.1}$$

$$Q^- = v_s\left[A_c(1/2 - \mu + \sigma C^o)^{1/2} + \frac{2}{3}\sum_w A_w(^o 1/2 - \mu - \sigma(C_w - C^o))^{3/2}\right] \tag{B6.2}$$

Since we are in the stack-dominated regime, the effective wind strength, $(C_w - C^o)\,\sigma$, must be small compared to unity to guarantee that the effective neutral level will be between the floor and the ceiling. Therefore, we can expand the terms containing σ and μ, assuming them to be small.

$$Q^+ = \sqrt{1/2}\; v_s\left[A_f(1 + \mu - \sigma C^0) + \sum_w A_w(\frac{1}{3} + \mu + \sigma(C_w - C^0))\right] \tag{B7.1}$$

$$Q^- = \sqrt{1/2}\; v_s\left[A_c(1 - \mu + \sigma C^0) + \sum_w A_w(\frac{1}{3} - \mu - \sigma(C_w - C^0)))\right] \tag{B7.2}$$

We have replaced the quantity C^o by C^0 to indicate that we are evaluating the internal pressure coefficient at low wind strengths.

Flow continuity requires that the infiltration and exfiltration be equal; applying this restriction to Eq. B7.1 and B7.2 gives:

$$A_f(1 + \mu) + \frac{1}{3}\sum_w A_w(1 + 3\mu) = A_c(1 - \mu) + \frac{1}{3}\sum_w A_w(1 - 3\mu) \tag{B8.1}$$

$$\sum_w A_w (C_w - C^0) = 1/2\, C^0 (A_c + A_f) \tag{B8.2}$$

Solving these two equations leads to expressions for μ and C^0.

$$\mu = \frac{A_c - A_f}{A_c + A_f + 2\sum_w A_w} \tag{B9.1}$$

$$C^0 = \frac{\sum_w A_w C_w}{\sum_w A_w + \frac{A_c + A_f}{2}} \tag{B9.2}$$

We have found that these two parameters assure flow continuity and, thus, that infiltration and exfiltration will be equal. To calculate the actual infiltration (in the stack regime) it does not matter which we use; therefore, we will use the average.

$$Q = 8^{-1/2}\, v_s\left[A_f(1+\mu) + A_c(1-\mu) + \frac{2}{3}\,(A_o-A_f-A_c) + \sigma C^0 A_o \mu\right] \tag{B10}$$

Neglecting terms of order μ^2 we get,

$$Q = 72^{-1/2}\, v_s\left[2\,A_o + A_f + A_c + 3\,\sigma\,C^0\,A_o\,(A_c - A_f)\right] \tag{B11}$$

where

A_o is the total leakage area $(\sum_w A_w + A_f + A_c)$

Wind Regime

In the wind-regime we assume that none of the effective neutral levels are between the floor and the ceiling ($1<\beta_j$ or $\beta_j<0$). In the stack regime we assumed the effective wind strength was small compared to unity; here we will assume the opposite. Extracting the wind-regime data from Table B1 and making the indicated replacements, we form Table B2, presenting simplified wind-regime infiltration values

We can find the internal pressure coefficient in the same manner as we did the stack effect (i.e. by requiring infiltration and exfiltration to balance). However, in the wind-regime the equations are non-linear and can only be solved numerically once values for shielding coefficients and leakage areas are known. Having found the internal pressure coefficient, we can find the infiltration by averaging the air flow out of the structure and the air flow into the structure.

$$Q = \frac{v}{2}\left[\sqrt{|C^\infty|}\,(A_c+A_f+\frac{\mu}{4\sigma C^\infty}(A_o+2A_f+2A_c))\right] + \frac{v}{2}\left[\sum_w A_w\sqrt{|(C_w - C^o)|}\,(1+\frac{\mu}{\sigma(C_w - C^\infty)})\right] \tag{B12.1}$$

$$= \frac{v}{2}\left[\sqrt{|C^\infty|}\,(A_c + A_f) + \sum_w A_w\sqrt{(C_w - C^\infty)}\right] + \frac{v\,\mu}{2\sigma}\left[\sum_w \frac{A_w}{\sqrt{|(C_w - C^\infty)|}} - \frac{(2A_o + A_f + A_c)}{2\sqrt{|C^\infty|}}\right] \tag{B12.2}$$

where

C^∞ is the internal shielding coefficient at high wind strength,

Now that we have expressions for the infiltration in the stack and wind-regimes, we must be able to reduce them to a level of simplicity commensurate with the results obtained from pressurization. To this purpose, we must make a few more approximations.

APPROXIMATION 5: Directional wind effects are unimportant

In any real structure, there are directional effects due to leakage distribution and shielding distribution. We are going to neglect such effects or, equivalently, assume that the wind direction changes enough in the time frame under consideration to average out any such effects.

If directional effects are unimportant, then we can simplify the various sums over shielding coefficients.

$$\sum_w A_w q_w = (A_o - A_c - A_f)\ \langle q_w \rangle \qquad \text{(B13)}$$

where

q_w is any quantity that must be summed over the walls,

$\langle q_w \rangle$ is the average value of that quantity and

$\sum_w A_w = A_o - A_f - A_c$

APPROXIMATION 6: The structure is typically shielded.

We will use numerical values for the external shielding parameters for a typical house of rectangular floor plan. This assumption combined with the previous one allows us to average over wind directions as well. If a particular structure has highly non-uniform shielding, then the dimensionless constants will retain their angular dependence.

We have chosen to use wind-tunnel values for a house of rectangular floor plan.[16]

APPROXIMATION 7: The internal pressure coefficient is constant

We have solved explicitly for the internal pressure coefficient at low wind strengths and we can solve numerically for the internal pressure coefficient at high wind strengths. If we do so, we find that they are roughly equal for any reasonable choice of C's and A's. We can then replace all of the internal pressure coefficients by a single value.

$$C^{\infty} = C^{0} = C^{o} \qquad \text{(B14)}$$

We can now rewrite the stack-regime and wind-regime equations by making a new definition to eliminate A_c and A_f.

$$R = \frac{A_c + A_f}{A_o} \qquad \text{(B15)}$$

Rewriting the two infiltration equations, we have:

$$Q_{stack} = 72^{-1/2} A_o v_s \ (2 + R) + 288^{-1/2} A_o \frac{v^2}{v_s} \mu C^o \qquad \text{(B16)}$$

$$Q_{wind} = \frac{1}{2} A_o v \sqrt{|C^o|}\ \left(R + (1-R) \left\langle \sqrt{|(C_w - C^o)|} \right\rangle + \right. \qquad \text{(B17)}$$

$$A_o \frac{v_s^2}{v} \mu \left[\frac{(1 - R)}{<\sqrt{|(C_w - C^o)|}>} - \frac{(1 + \frac{R}{2})}{\sqrt{|C^o|}} \right]$$

APPROXIMATION 8: The infiltration is independent of the sign of ΔT

In the preceding derivation we assumed that the stack pressure was positive (*i.e.*, that inside is greater than outside temperature). If the reverse is true, the only change in these equations is a sign reversal of μ; for cooling loads μ should be replaced by $-\mu$ in all the above equations. In both equations this asymmetric term is quite small; therefore, we will set these terms to zero.

$$Q_{stack} = 72^{-1/2} A_o v_s (2 + R) \quad \text{(B18.1)}$$

$$Q_{wind} = 1/2 A_o v \left[\sqrt{|C^o|} R + (1-R) <\sqrt{|(C_w - C^o)|}> \right] \quad \text{(B18.2)}$$

From the wind-tunnel data we can calculate the terms involving the shielding parameters.

$$C^o = -.21 \quad \text{(B19.1)}$$

$$< \sqrt{|(C_w - C^o)|} > = 0.68 \quad \text{(B19.2)}$$

We now insert the numerical values into the equations and define two dimensionless parameters f_s and f_w.

$$f_s = \frac{2 + R}{9} \quad \text{(20.}$$

$$f_w = \frac{3 - R}{9} \quad \text{(B20.}$$

These expressions are accurate to two significant figures.

Combining these terms yields expressions for the stack and wind infiltration.

$$Q_{stack} = f_s A_o v_s \quad \text{(B21.1)}$$

$$Q_{wind} = f_w A_o v \quad \text{(B21.2)}$$

COMBINING WIND AND STACK REGIMES

We have an expression for the infiltration in the stack regime and an expression for infiltration in the wind-regime, but we have no adequate expression for the intermediate case. Although the intermediate case will no doubt be very complicated and site-specific, we will assume that one of the two equations will adequately describe the situation. We shall use the larger of the two infiltration values at all times.

$$Q(\Delta T, v) = A_o \, MAX(f_s v_s, f_w v) \tag{B22}$$

<u>where</u>

$Q(\Delta T,v)$ is the instantaneous infiltration.

There is a wind speed at which the stack effect and wind effect become equal. Above that wind speed, the wind effect dominates while below, the stack effect dominates. At the equilibrium wind speed,

$$f_w v = f_s v_s = f_s \sqrt{2gH \frac{\Delta T}{T}} \tag{B23}$$

Depending on the value of R, the equilibrium wind speed may be anywhere from 2/3 v_s to v_s.

NOMENCLATURE

A	effective leakage area [m^2]
A_o	total leakage area ($\sum_w A_w + A_f + A_c$)
c	subscript indicating the ceiling
C	(wind pressure) shielding coefficient
C^o	internal (wind) pressure coefficient
C^∞	internal pressure coefficient at high wind strength
f_s	stack-effect factor
f_s^*	reduced-stack effect factor [$m/s/\sqrt{^oK}$]
f_w	wind-effect factor
f_w^*	reduced wind-effect factor
g	acceleration of gravity [9.8 m/sec^2]
h	height variable [m]
H	height of the ceiling above grade [m]
H′	height of the wind measurement
j	index to denote each face of the structure
L	semi-empirical constant used in empirical fits to leakage data
n	semi-empirical constant used in empirical fits to leakage data
P_{st}	stagnation pressure ($\frac{1}{2}\rho v^2$) [Pa]
P_s	stack pressure ($\rho g H \frac{\Delta T}{T}$)
ΔP	applied pressure difference.
ΔP_j^w	exterior pressure rise due to the wind
ΔP_o	internal pressure change
Q	is air flow [m^3/sec]
$Q(\Delta T,v)$	instantaneous infiltration
Q_{stack}	infiltration in the stack regime
Q_{wind}	infiltration in the wind regime
R	fraction of leakage area combined in floor and ceiling

NOMENCLATURE

T	inside temperature [^oK]
ΔT	inside-outside temperature difference
v	wind speed at ceiling height [m/sec]
v^*	reduced wind speed
v_o	wind speed at standard (terrain) conditions
v_s	critical wind speed
v_s^*	reduced critical wind speed
v'	measured wind speed
w	index to denote the walls of the structure
α	constant that depends on terrain class (see tables above)
β	normalized height
β_j	effective neutral level of the jth face
β^o	neutral level
γ	constant dependent on terrain class (see tables above)
μ	fraction shift in the neutral level from the mid-point
ρ	density of air [1.2 kg/m^3]
σ	wind strength
$\pm$	indicates depressurization/pressurization or infiltration/exfiltration respectively

REFERENCES

1. Bahnfleth, D.R., Moseley, D.T. and Harris, W.S., "Measurement of Infiltration in Two Residences," ASHRAE TRANSACTIONS, 63, 439-452, 1957.

2. Dick, J.B., and Thomas, D.A., "Ventilation Research in Occupied Houses," J. Inst. Heat. Vent. Eng., 19, 306-332, 1951.

3. Malik, N., "Field Studies of Dependence of Air Infiltration on Outside Temperature and Wind," Energy and Buildings, 1, 281-292, 1978.

4. Grimsrud,D.T., Sherman, M.H., Diamond, R.C., Condon, P.E., and Rosenfeld, A.H., "Infiltration-Pressurization Correlations: Detailed Measurements on a California House," ASHRAE TRANSACTIONS, 85, 1:851-865, 1979. LBL Report No. 7824 (1978)

5. Etheridge, D.W., "Crack Flow Equations and Scale Effect," Building & Environment, 12, 181-189, 1977.

6. Sherman, M.H., Grimsrud, D.T., and Sonderegger, R.C., "Low Pressure Leakage Function of a Building," Proc. ASHRAE-DOE Conference on the Thermal Performance of the Exterior Envelopes of Buildings, Orlando, Florida, December 1979. LBL Report No. 9162 (1979)

7. Blomsterberg, A.K., and Harrje,D.T. , "Approaches to Evaluation of Air Infiltration Energy Losses in Buildings," ASHRAE TRANSACTIONS, 85, 1:797-815, 1979.

8. Grimsrud, D.T., Sherman, M.H., Diamond, R.C., and Sonderegger, R.C., "Air Leakage, Surface Pressures and Infiltration Rates in Houses," Proc. of the Second International CIB Symposium, Copenhagen, Denmark, May 1979, LBL Report No. 8828 (1979)

9. Harrje, D.T., Blomsterberg, A.K., and Persily, A., "Reduction of Air Infiltration due to Window and Door Retrofits in an Older Home," Princeton University/Center for Environmental Studies Report No. 85, 1979.

10. Grimsrud, D.T., Sherman, M.H., Blomsterberg, A.K., and Rosenfeld, A.H., "Infiltration and Air Leakage Comparisons: Conventional and Energy Efficient Housing Designs," Presented at the International Conference on Energy Use Management, Los Angeles, October 1979. LBL Report No. 9157 (1979)

11. Johns-Manville Research and Development Center, "Demonstration of Energy Conservation through Reduction of Air Infiltration in Electrically Heated Houses," RP 1351-1, 1979.

12. Tamura, G.T., "The Calculation of House Infiltration Rates," ASHRAE TRANSACTIONS, 85, 1:58-71, 1979.

13. Sherman, M.H., Grimsrud, D.T., and Diamond, R.C., "Infiltration-Pressurization Correlation: Surface Pressures and Terrain Effects," ASHRAE TRANSACTIONS, 85, 2:458-479, 1979. LBL Report No.8785 (1979)

14. European Convention for Constructional Steelwork, "Recommendations for the Calculation of Wind Effects on Buildings and Structures", Technical General Secretariat, Brussels, Belgium September 1978.

15. Kim, S., Mehta, K.C., "Full Scale Measurements on a Flat Roof Area," Proceedings of the Fifth Int. Conf. Wind Engineering, Boulder, Colorado, July 1979.

16. Akins, R.E., Peterka, J.A., and Cermak, J.E., "Average Pressure Coefficients for Rectangular Buildings," Proceedings of the Fifth Int. Conf. Wind Engineering, Boulder, Colorado, July 1979.

ACKNOWLEDGMENT

The authors would like to thank Fannie Walkin for her invaluable guidance in simplifying this derivation.

Table 1 Reduced Stack Parameter(f_s^*)

H	R .05	.10	.15	.20	.25	.30	.35	.40	.45	.50
0.5	.042	.043	.044	.045	.046	.047	.048	.049	.050	.051
1.0	.059	.060	.062	.063	.064	.066	.067	.069	.070	.072
1.5	.072	.074	.075	.077	.079	.081	.082	.084	.086	.088
2.0	.083	.085	.087	.089	.091	.093	.095	.097	.099	.101
2.5	.093	.095	.097	.100	.102	.104	.106	.109	.111	.113
3.0	.102	.104	.107	.109	.112	.114	.117	.119	.122	.124
3.5	.110	.113	.115	.118	.121	.123	.126	.129	.131	.134
4.0	.117	.120	.123	.126	.129	.132	.135	.137	.140	.143
4.5	.125	.128	.131	.134	.137	.140	.143	.146	.149	.152
5.0	.131	.134	.138	.141	.144	.147	.150	.154	.157	.160
5.5	.138	.141	.144	.148	.151	.154	.158	.161	.165	.168
6.0	.144	.147	.151	.154	.158	.161	.165	.168	.172	.175
6.5	.150	.153	.157	.161	.164	.168	.172	.175	.179	.183
7.0	.155	.159	.163	.167	.170	.174	.178	.182	.186	.189
7.5	.161	.165	.169	.173	.176	.180	.184	.188	.192	.196
8.0	.166	.170	.174	.178	.182	.186	.190	.194	.198	.203
8.5	.171	.175	.180	.184	.188	.192	.196	.200	.205	.209
9.0	.176	.180	.185	.189	.193	.198	.202	.206	.211	.215
9.5	.181	.185	.190	.194	.199	.203	.207	.212	.216	.221
10.0	.186	.190	.195	.199	.204	.208	.213	.217	.222	.226

Table 2.1 Reduced Wind Parameter (f_w^*) for Terrain Class 1

H	R .05	.10	.15	.20	.25	.30	.35	.40	.45	.50
0.5	.243	.239	.235	.231	.226	.222	.218	.214	.210	.206
1.0	.260	.256	.252	.247	.243	.238	.234	.229	.225	.221
1.5	.271	.267	.262	.257	.253	.248	.244	.239	.234	.230
2.0	.279	.274	.270	.265	.260	.255	.251	.246	.241	.236
2.5	.285	.281	.276	.271	.266	.261	.256	.251	.247	.242
3.0	.291	.286	.281	.276	.271	.266	.261	.256	.251	.246
3.5	.295	.290	.285	.280	.275	.270	.265	.260	.255	.250
4.0	.299	.294	.289	.284	.279	.274	.269	.264	.259	.253
4.5	.303	.297	.292	.287	.282	.277	.272	.267	.262	.256
5.0	.306	.301	.295	.290	.285	.280	.275	.270	.264	.259
5.5	.309	.304	.298	.293	.288	.283	.277	.272	.267	.262
6.0	.311	.306	.301	.296	.290	.285	.280	.275	.269	.264
6.5	.314	.309	.303	.298	.293	.287	.282	.277	.271	.266
7.0	.316	.311	.306	.300	.295	.289	.284	.279	.273	.268
7.5	.318	.313	.308	.302	.297	.291	.286	.281	.275	.270
8.0	.321	.315	.310	.304	.299	.293	.288	.283	.277	.272
8.5	.322	.317	.312	.306	.301	.295	.290	.284	.279	.273
9.0	.324	.319	.313	.308	.302	.297	.291	.286	.280	.275
9.5	.326	.321	.315	.310	.304	.298	.293	.287	.282	.276
10.0	.328	.322	.317	.311	.306	.300	.294	.289	.283	.278

Table 2.2 Reduced Wind Parameter (f_w^*) for Terrain Class 2

H	R .05	.10	.15	.20	.25	.30	.35	.40	.45	.50
0.5	.209	.206	.202	.199	.195	.191	.188	.184	.181	.177
1.0	.232	.228	.224	.220	.216	.212	.208	.205	.201	.197
1.5	.247	.242	.238	.234	.230	.226	.222	.217	.213	.209
2.0	.257	.253	.249	.244	.240	.236	.231	.227	.223	.218
2.5	.266	.262	.257	.253	.248	.244	.239	.235	.230	.226
3.0	.274	.269	.264	.260	.255	.250	.246	.241	.237	.232
3.5	.280	.275	.271	.266	.261	.256	.252	.247	.242	.237
4.0	.286	.281	.276	.271	.266	.261	.257	.252	.247	.242
4.5	.291	.286	.281	.276	.271	.266	.261	.256	.251	.246
5.0	.295	.290	.285	.280	.275	.270	.265	.260	.255	.250
5.5	.300	.295	.290	.284	.279	.274	.269	.264	.259	.254
6.0	.304	.298	.293	.288	.283	.278	.273	.268	.262	.257
6.5	.307	.302	.297	.292	.286	.281	.276	.271	.266	.260
7.0	.311	.305	.300	.295	.290	.284	.279	.274	.269	.263
7.5	.314	.309	.303	.298	.293	.287	.282	.277	.271	.266
8.0	.317	.312	.306	.301	.295	.290	.285	.279	.274	.269
8.5	.320	.314	.309	.304	.298	.293	.287	.282	.277	.271
9.0	.323	.317	.312	.306	.301	.295	.290	.284	.279	.273
9.5	.325	.320	.314	.309	.303	.298	.292	.287	.281	.276
10.0	.328	.322	.317	.311	.306	.300	.294	.289	.283	.278

Table 2.3 Reduced Wind Parameter (f_w^*) for Terrain Class 3

H	R .05	.10	.15	.20	.25	.30	.35	.40	.45	.50
0.5	.180	.177	.174	.171	.168	.165	.162	.159	.156	.153
1.0	.207	.203	.200	.196	.193	.189	.186	.182	.179	.175
1.5	.224	.220	.217	.213	.209	.205	.201	.198	.194	.190
2.0	.238	.234	.230	.225	.221	.217	.213	.209	.205	.201
2.5	.248	.244	.240	.236	.232	.227	.223	.219	.215	.211
3.0	.258	.253	.249	.245	.240	.236	.231	.227	.223	.218
3.5	.266	.261	.257	.252	.248	.243	.239	.234	.230	.225
4.0	.273	.268	.264	.259	.254	.250	.245	.241	.236	.231
4.5	.279	.275	.270	.265	.260	.256	.251	.246	.242	.237
5.0	.285	.281	.276	.271	.266	.261	.256	.251	.247	.242
5.5	.291	.286	.281	.276	.271	.266	.261	.256	.251	.246
6.0	.296	.291	.286	.281	.276	.271	.266	.261	.256	.251
6.5	.301	.296	.291	.285	.280	.275	.270	.265	.260	.255
7.0	.305	.300	.295	.290	.285	.279	.274	.269	.264	.259
7.5	.309	.304	.299	.294	.288	.283	.278	.273	.267	.262
8.0	.313	.308	.303	.298	.292	.287	.282	.276	.271	.266
8.5	.317	.312	.307	.301	.296	.290	.285	.280	.274	.269
9.0	.321	.316	.310	.305	.299	.294	.288	.283	.277	.272
9.5	.324	.319	.313	.308	.302	.297	.291	.286	.280	.275
10.0	.328	.322	.317	.311	.306	.300	.294	.289	.283	.278

Table 2.4 Reduced Wind Parameter (f_w^*) for Terrain Class 4

H	R									
	.05	.10	.15	.20	.25	.30	.35	.40	.45	.50
0.5	.155	.152	.150	.147	.144	.142	.139	.137	.134	.131
1.0	.184	.181	.178	.175	.172	.169	.166	.162	.159	.156
1.5	.204	.201	.197	.194	.190	.187	.183	.180	.176	.173
2.0	.219	.215	.212	.208	.204	.201	.197	.193	.189	.186
2.5	.232	.228	.224	.220	.216	.212	.208	.204	.200	.196
3.0	.243	.238	.234	.230	.226	.222	.218	.214	.210	.206
3.5	.252	.248	.244	.239	.235	.231	.226	.222	.218	.214
4.0	.261	.256	.252	.247	.243	.239	.234	.230	.225	.221
4.5	.268	.264	.259	.255	.250	.246	.241	.237	.232	.228
5.0	.276	.271	.266	.262	.257	.252	.248	.243	.238	.234
5.5	.282	.277	.273	.268	.263	.258	.254	.249	.244	.239
6.0	.288	.284	.279	.274	.269	.264	.259	.254	.249	.244
6.5	.294	.289	.284	.279	.274	.269	.264	.259	.254	.249
7.0	.300	.295	.290	.285	.279	.274	.269	.264	.259	.254
7.5	.305	.300	.295	.290	.284	.279	.274	.269	.264	.259
8.0	.310	.305	.299	.294	.289	.284	.278	.273	.268	.263
8.5	.315	.309	.304	.299	.293	.288	.283	.277	.272	.267
9.0	.319	.314	.308	.303	.298	.292	.287	.281	.276	.271
9.5	.324	.318	.313	.307	.302	.296	.291	.285	.280	.274
10.0	.328	.322	.317	.311	.306	.300	.294	.289	.283	.278

Table 2.5 Reduced Wind Parameter (f_w^*) for Terrain Class 5

H	R									
	.05	.10	.15	.20	.25	.30	.35	.40	.45	.50
0.5	.133	.131	.129	.127	.124	.122	.120	.118	.115	.113
1.0	.164	.161	.159	.156	.153	.150	.148	.145	.142	.139
1.5	.186	.182	.179	.176	.173	.170	.167	.164	.160	.157
2.0	.202	.199	.195	.192	.189	.185	.182	.178	.175	.171
2.5	.216	.213	.209	.205	.202	.198	.194	.191	.187	.183
3.0	.228	.225	.221	.217	.213	.209	.205	.201	.197	.194
3.5	.239	.235	.231	.227	.223	.219	.215	.211	.207	.203
4.0	.249	.245	.241	.236	.232	.228	.224	.219	.215	.211
4.5	.258	.254	.249	.245	.240	.236	.232	.227	.223	.219
5.0	.266	.262	.257	.253	.248	.244	.239	.235	.230	.226
5.5	.274	.269	.265	.260	.255	.251	.246	.241	.237	.232
6.0	.281	.276	.272	.267	.262	.257	.253	.248	.243	.238
6.5	.288	.283	.278	.273	.269	.264	.259	.254	.249	.244
7.0	.295	.290	.285	.280	.275	.270	.265	.260	.255	.250
7.5	.301	.296	.290	.285	.280	.275	.270	.265	.260	.255
8.0	.307	.301	.296	.291	.286	.281	.275	.270	.265	.260
8.5	.312	.307	.302	.296	.291	.286	.280	.275	.270	.265
9.0	.318	.312	.307	.301	.296	.291	.285	.280	.275	.269
9.5	.323	.317	.312	.306	.301	.295	.290	.284	.279	.274
10.0	.328	.322	.317	.311	.306	.300	.294	.289	.283	.278

Table 3: Test Site Parameters					
HOUSE ID	Ref No.	A_o cm^2	f_w^*	f_s^* $m/s/^oC^{1/2}$	Vol m^3
Ivanhoe	10	100	.26	.12	480
Nogal	10	960	.21	.10	290
Telemark	10	140	.26	.12	480
Torey Pines	10	200	.30	.14	480
R-10	11	330	.20	.09	233
T1	12	330	.18	.13	337
T2	12	680	.22	.11	433
Haven	10	770	.21	.11	230
Purdue	10	855	.21	.11	240
Neilson	10	1275	.20	.13	250
V1	10	560	.20	.12	270
V2	10	630	.19	.12	270
Fels	9	1480	.26	.15	470
San Carlos	10	845	.18	.11	145
Southampton	10	1640	.22	.16	1000

Table 4: Predicted Infiltration vs Measured Infiltration								
HOUSE ID	v'	$\delta v'$	ΔT	δT	Q_p	δQ_p	Q_m	δQ_m
Ivanhoe	6.0	1.0	26	0	79	13	53	4
Nogal	1.7	0.1	3	1	114	4	123	12
Telemark	4.0	1.0	25	1	52	7	50	12
Torey Pines	7.2	1.0	19	1	156	10	180	23
R-10	2.0	0.1	28	1	72	2	77	7
T1	2.7	1.3	16	15	76	15	69	13
T2	2.7	2.0	15	15	149	110	139	80
Haven	3.0	2.0	8	4	175	60	68	42
Purdue	2.7	1.2	9	1	164	73	133	19
Neilson	1.7	0.3	5	1	156	28	173	13
V1	2.1	0.1	6	1	87	10	86	3
V2	3.3	1.1	7	2	142	44	125	48
Fels	4.0	2.0	16	4	554	140	355	175
San Carlos	1.7	0.2	0	1	93	11	114	26
Southampton	1.0	0.1	0	1	130	7	250	60

Table A1: Terrain Parameters for Standard Terrain Classes			
Class	γ	α	Description
I	0.10	1.30	ocean or other body of water with at least 5km of unrestricted expanse
II	0.15	1.00	flat terrain with some isolated obstacles (buildings or trees well separated from each other
III	0.20	0.85	rural areas with low buildings, trees, etc.
IV	0.25	0.67	urban, industrial or forest areas
V	0.35	0.47	center of large city (Manhattan)

Table A2: Infiltration Through Each Face			
Direction	Condition	Location	Expression
Infiltration	$\beta_j < 0$	floor	0
		wall	0
		ceiling	0
	$0 < \beta_j < 1$	floor	$L\,P_s^n\,\beta_j^n$
		wall	$\frac{L\,P_s^n}{n+1}\,\beta_j^{n+1}$
		ceiling	0
	$1 < \beta_j$	floor	$L\,P_s^n\,(\beta_j-1)^n$
		wall	$\frac{L\,P_s^n}{n+1}\left[\beta_j^{n+1} - (\beta_j-1)^{n+1}\right]$
		ceiling	$L\,P_s^n\,\beta_j^n$
Exfiltration	$\beta_j < 0$	floor	$L\,P_s^n\,(-\beta_j)^n$
		wall	$\frac{L\,P_s^n}{n+1}\left[(1-\beta_j)^{n+1} - (-\beta_j)^{n+1}\right]$
		ceiling	$L\,P_s^n\,(1-\beta_j)^n$
	$0 < \beta_j < 1$	floor	0
		wall	$\frac{L\,P_s^n}{n+1}\,(1-\beta_j)^{n+1}$
		ceiling	$L\,P_s^n\,(1-\beta_j)^n$
	$1 < \beta_j$	floor	0
		wall	0
		ceiling	0

Table B1: Infiltration Through Each Face

Direction	Condition	Location	Expression
Infiltration	$\beta_j < 0$	floor	0
		wall	0
		ceiling	0
	$0 < \beta_j < 1$	floor	$A_f \, v_s \sqrt{\beta_f}$
		wall	$\frac{2}{3} A_w \, v_s \, \beta_w^{3/2}$
		ceiling	0
	$1 < \beta_j$	floor	$A_f \, v_s \sqrt{\beta_f - 1}$
		wall	$\frac{2}{3} A_w \, v_s \left[\beta_w^{3/2} - (\beta_w - 1)^{3/2}\right]$
		ceiling	$A_c \, v_s \sqrt{\beta_c}$
Exfiltration	$\beta_j < 0$	floor	$A_f \, v_s \sqrt{-\beta_f}$
		wall	$\frac{2}{3} A_w \, v_s \left[(1-\beta_w)^{3/2} - (-\beta_w)^{3/2}\right]$
		ceiling	$A_c \, v_s \sqrt{1-\beta_c}$
	$0 < \beta_j < 1$	floor	0
		wall	$\frac{2}{3} A_w \, v_s \, (1-\beta_w)^{3/2}$
		ceiling	$A_c \, v_s \sqrt{1-\beta_c}$
	$1 < \beta_j$	floor	0
		wall	0
		ceiling	0

Table B2: Wind Regime Infiltration Values

Face	Infiltration/Exfiltration
floor	$v \, A_f \sqrt{\lvert C^o \rvert} \, \left(1 - \frac{2\mu - 1}{4\sigma C^o}\right)$
wall	$v \sum_w A_w \sqrt{\lvert (C_w - C^o) \rvert} \, \left(1 + \frac{\mu}{\sigma(C_w - C^o)}\right)$
ceiling	$v \, A_c \sqrt{\lvert C^o \rvert} \, \left(1 - \frac{2\mu + 1}{4\sigma C^o}\right)$

Defining Relations for Figures

$$R = \frac{A_c + A_f}{A_o}$$

$$f_w = \frac{3 - R}{9}$$

$$f_s = \frac{2 + R}{9}$$

$$v = v' \left[\frac{\alpha \left(\frac{H}{10} \right)^{\gamma}}{\alpha' \left(\frac{H'}{10} \right)^{\gamma'}} \right]$$

$$v^* = f_w \, v = v' \, f_w^*$$

$$f_w^* = \frac{3 - R}{9} \left[\frac{\alpha \left(\frac{H}{10} \right)^{\gamma}}{\alpha' \left(\frac{H'}{10} \right)^{\gamma'}} \right]$$

$$v_s^* = f_s \, v_s = \sqrt{\Delta T} \; f_s^*$$

$$f_s^* = \frac{2 + R}{9} \sqrt{\frac{2 \, g \, H}{T}}$$

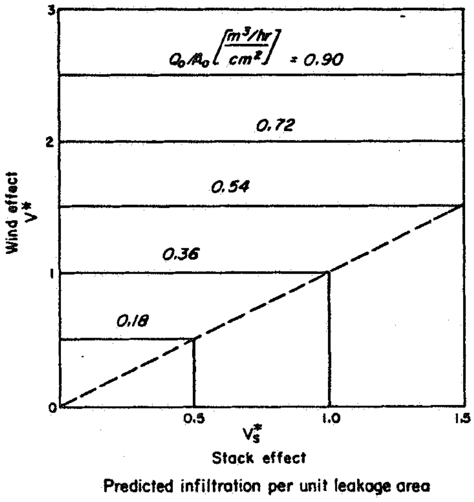

Fig. 1 Lines of constant infiltration as a function of the 2 reduced velocities: the dashed line separates the stack-dominated and wind-dominated regimes. (Refer to "Symbol Table" and "Defining Relations" preceding the figures.)

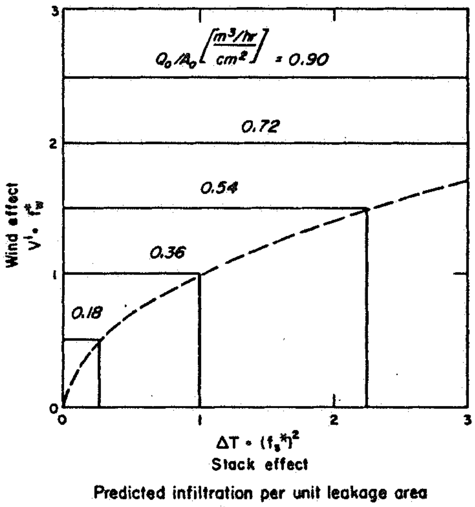

Fig. 2 Lines of constant infiltration as a function of wind speed and temperature difference: the dashed line separates the stack-dominated and wind-dominated regimes. (Refer to "Defining Relations" preceding the figures. This figure contains essentially the same information as Fig. 1, but expresses it in different variables.)

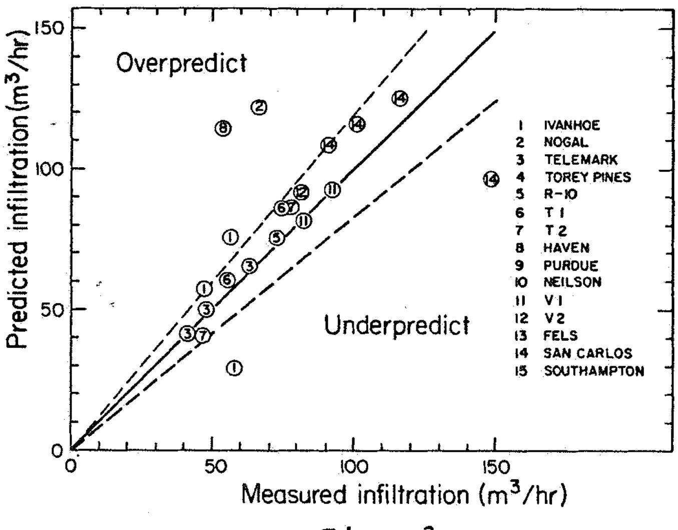

Fig. 3

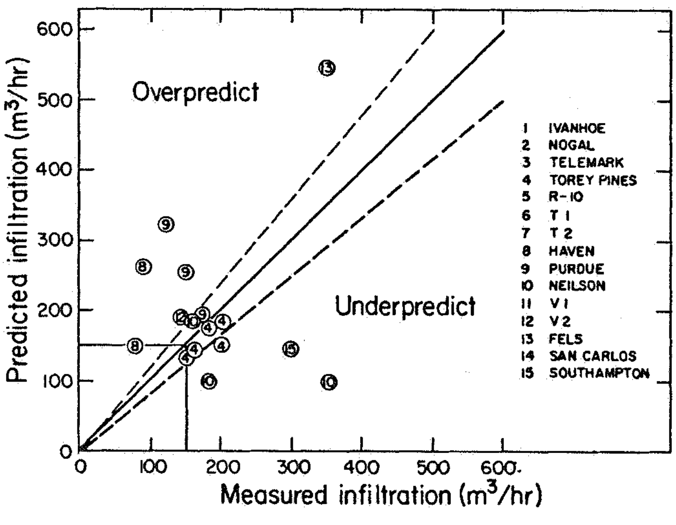

Fig. 4

Fig. 3 A graph of the predicted vs measured infiltration points for all data points that had both predicted and measured infiltration values of less than 150 m^3/h: the solid line is the locus of points that represents perfect agreement; the dashed lines define an area of acceptable agreement based on the measurement uncertainties only.

Fig. 4 A graph of the predicted vs measured infiltration points not included on the previous graph: the box in the lower left hand corner is the range of the previous graph; the solid line is the locus of points that represents perfect agreement; the dashed lines define an area of acceptable agreement based on the measurement uncertainties only.

DISCUSSION

JEAN LeBRUN, Prof., Univ. of Liege, Liege, Belgium: In the infiltration measurements, it is difficult to identify correctly the micro-climate to which the building is really submitted. What complementary measurements could we make (local velocity, wall measurements)?

MAX SHERMAN: While it is true that the micro-climate in the immediate vicinity of the structure determines the driving forces of infiltration, it is impractical to base a model of infiltration on these parameters, if we wish to make use of this model in the field. We have, therefore, used the local (but not micro) weather conditions as our inputs to the model.

LeBRUN: If these measurements are not satisfactory, I would suggest the following: Those who analyze building air infiltrations should use a "reference model" in the vicinity of the building being considered, e.g. a small cube with calibrated orifices that could be eventually tested under laboratory conditions. Continuous air infiltration measurements on the reference model would constitute a checking of our understanding of the phenomena and validity of our theoretical and experimental procedures (e.g., the interpretation of the micro-climate). There is no hope of significant results in the building if we are not able to understand what happens in the reference model. We are already applying this methodology in Belgium for the heating energy analysis of buildings.

SHERMAN: It is, however, important in the model <u>development</u> stage to be able to connect the local weather to the micro-climate and the micro-climate to the infiltration. For this purpose, we have built a Mobile Infiltration Test Unit (MITU) which is fully instrumented to measure weather, infiltrations, surface pressures and interior conditions. We expect to validate our model using MITU and supply data to the Air Infiltrations Center in Bracknell, U.K., for general use.